ISSN 0208-7774 TRIBOLOGIA 4/2021 p. 7–14
DOI: 10.5604/01.3001.0015.8364

Kinga CHRONOWSKA-PRZYWARA*

ANALYSIS OF DEFORMATION AND FORMS OF DESTRUCTION OF COATING-SUBSTRATE SYSTEMS

ANALIZA DEFORMACJI I FORM NISZCZENIA UKŁADU POWŁOKA–PODŁOŻE

Key words: contact mechanics, fracture toughness, deformation, coatings.

Abstract: The paper presents the results of fracture testing of a coating-substrate system subjected to a concentrated contact load and during a scratch test. A diamond indenter with rounding radii in the range 20-500 μm was used under the tests. Systems with CrN coatings in the range of 1 to 5 μm applied to austenitic steel X5CrNi18-10 were analysed. In the paper, the effect of coating thickness on deformation and fracture of the coating and substrate in the load range of 1 and 3 N is analysed. Cohesion and adhesion sites of the coating to the substrate were determined. Optical profilometer images, scanning microscope images, and Micro Combi Tester images – CSM Instruments were used to analyse Lc1, Lc2, and crack locations. It was observed that, as the indenter radius increases, cracks in the coating-substrate system develop at increasing loads. Average critical forces are also higher with indenters of 200–500 μm. In the case of indentation only, with the indenter's radius of 500 um, it is 750 Nm for the thinnest 1 μm coating and 1750 Nm for the 5.2 μm coating.

Słowa kluczowe: mechanika kontaktu, odporność na pękanie, deformacja, powłoka.

Streszczenie: W artykule przedstawiono wyniki badań pękania układu powłoka–podłoże poddanych obciążeniu działającym w styku skoncentrowanym oraz podczas testu zarysowania. Do badań użyto diamentowego wgłębnika o promieniach zaokrąglenia z zakresu 20–500 μm. Analizowano układy z powłokami CrN w zakresie od 1 do 5 μm nałożone na stal austenityczną X5CrNi18-10. W artykule analizowano wpływ grubości powłok na deformacje i pękanie powłoki i podłoża w zakresie obciążenia 1 i 3 N. Wyznaczono miejsca kohezji i adhezji powłoki do podłoża. Do analizy Lc1, Lc2 oraz lokalizacji pęknięć użyto obrazów z profilometru optycznego, zdjęć z mikroskopu skaningowego i zdjęć z Micro Combi Testera – CSM Instruments. W wyniku przeprowadzonych badań zauważono, że wraz ze wzrostem promieniem zaokrąglenia wgłębnika, pęknięcia układu powłoka–podłoże powstają przy coraz większych obciążeniach. Średnie wartości sił krytycznych również jest większe przy stosowaniu wgłębników 200–500 μm. W przypadku samej indentacji przy promieniu wgłębnika 500 μm wynosi 1 μm, 750 Nm, natomiast dla powłoki 5,2 μm 1750 Nm.

INTRODUCTION

Currently in the world, the widespread use of coatings, especially for highly loaded machine elements is so large that manufacturers are facing the need to improve their properties. The main goal is to reduce friction during contact of two interacting parts and cracking of surfaces causing the weakening of the structure of friction units. To meet the expectations, coatings have been applied on surfaces all over the world for over 40 years. Most often single coatings or multi-layer coating with different properties are applied alternately (**Fig. 1**). A huge development in the field of coating manufacturing can be observed on the world market **[L. 1, 2]**.

Some of the most commonly used methods of producing even newer coatings are the

* ORCID: 0000-0003-3510-4443. AGH University of Science and Technology, Faculty of Mechanical Engineering and Robotics, Mickiewicza Ave. 30, 30-059 Cracow, Poland, e-mail: chronows@agh.edu.pl.

Physical Vapour Deposition (PVD) method and the Chemical Vapour Deposition (CVD) method. Due to these methods of coating application, the surface durability of materials used for machine elements operating in difficult conditions has been effectively increased for many years **[L. 3–5]**.

By choosing the proper coating and the way it is applied, the reliability of machine parts made of materials with reduced functional properties can be significantly increased. Thanks to that, usually cheaper materials are used, which, after applying coatings, gain better exploitation properties. This often leads to a reduction in mass at the expense of an increase in energy cost for its manufacture with the same strength properties.

However, despite the widespread use of coatings, there is no complete vision of the failure of the coating-substrate system. Deformations, plastic deformations, and cracking in such systems are determined by coating thickness, the modulus of elasticity, resistance to brittle fracture of coating and substrate materials, and hardness. Determination of permissible loads at which cracking of coatings occurs is most often carried out experimentally. Diagnosis of the form of destruction of such systems allows one to significantly extend the service life of the cooperating tribological pairs. The failure occurs due to abrasive wear without the occurrence of significant cracks and the separation of the coating from the substrate lead to a faster or sudden destruction of the system **[L. 6–8]**.

Increasing the indenter load leads to bending of the coating and thus to tensile stresses on the coating surface immediately behind the indenter contact area and in the indenter axis of symmetry at the coating-substrate interface (**Fig. 2**) **[L. 2]**. Due to determining the permissible loads, it is possible to avoid various forms of wear of the coating-substrate system, taking into account both the stresses at the indenter contact area and at the coating-substrate interface. The solution of this problem is the subject of this paper.

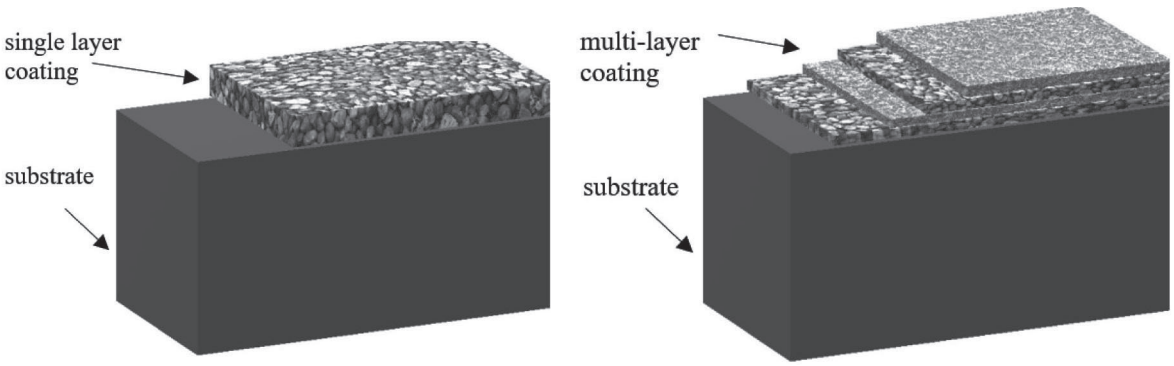

Fig. 1. Illustration of structure for the coating-substrate system: a) single-layer coating, b) multi-layer coating
Rys. 1. Obraz struktury układu powłoka–podłoże: a) powłoka jednowarstwowa, b) powłoka wielowarstwowa

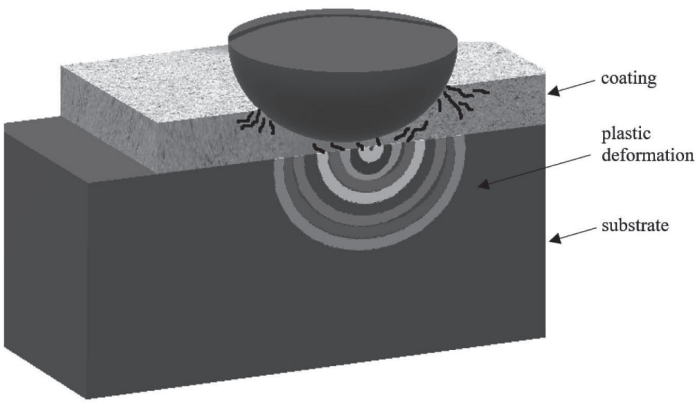

Fig. 2. Graphical representation of deformation for the coating-substrate systems under the influence of loads acting in concentrated contact during indentation
Rys. 2. Graficzne przedstawienie deformacji układów powłoka–podłoże pod wpływem obciążeń działających w skoncentrowanym kontakcie podczas indentacji

RESEARCH METHODS

One of the many problems of applying coatings to machine and equipment components, especially in heavy industry, is the selection of appropriate friction units. There is still no adequate knowledge base on the properties of the coatings used. This is mainly due to the fact that even commonly used single coatings such as TiN, CrN, a-C:H, or nanocomposite nc-Cr2C/a-C:H show significantly different properties when produced by different techniques. In addition, the difference in properties is due to the difference in substrates used. Therefore, it is necessary to continuously analyse the tribological and mechanical properties of coatings in order to get the optimal coating for a specific application. For this purpose, it is best to perform a complete failure analysis of complex coating-substrate systems under load acting in concentrated contact **[L. 14]**.

CrN coatings with thicknesses t = 1, 2, 4.1, and 5.2 μm were tested. The substrate X20Cr13 from ferritic steel was used to model the coating-substrate system. The coatings were deposited using the Physical Vapour Deposition (PVD) method, which involves the physical deposition of coatings from the gas phase at a pressure of $10\text{-}10^5$ Pa. This method uses the phenomenon of cathodic sputtering in a vacuum and the ionization of gases and metal vapours or phases from plasma. Indentation tests were performed on a Micro-Combi- Tester. An indenter with Rockwell geometry and rounding radii of 20, 50, 200, and 500 μm was used. Measurements were performed with constant increasing of the indenter load (**Fig. 3**).

Each combination of tests parameters was examined six times. The critical load values L_{c1} and L_{c2} were determined by analysing the acoustic emission signal and the imprint image after the test from an optical microscope with x200 magnification.

Material parameters of the coating, substrate, and indenter were taken to perform deformation and fracture analysis of the coating-substrate system as follows:

- Coating: Young's modulus E = 210 GPa, yield strength Re = 800 MPa, Poisson's number ϑ = = 0.3,
- Substrate: Young's modulus E = 420 GPa, Poisson's number ϑ = 0.25, and
- Indenter: yield strength E = 1041 GPa Poisson number ϑ = 0.07.

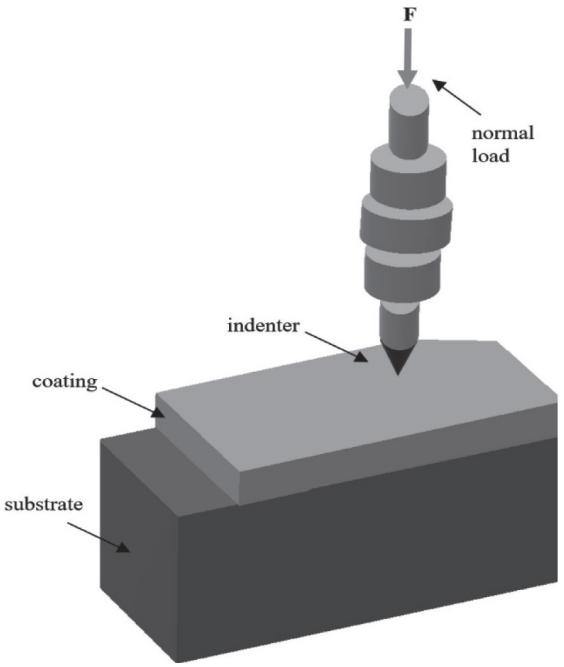

Fig. 3. Scheme of the system loading the test sample in the indentation test

Rys. 3. Schemat układu obciążającego badaną próbkę w teście indentacyjnym

EXPERIMENTAL RESULTS

Analysis of the results of the tests performed for the coating-substrate system in concentrated contact allows to determining the average value of the critical forces for the tested systems (**Fig. 4**). The following diagrams are presented for six coating-substrate systems and four indenters with different rounded tip geometries. After comparing the results for the different indenter rounded tips selected for the tests, it can be seen that, as the coating thickness increases, the average value of the critical forces at which deformations occur increases (**Fig. 4**) For the coating with 1 um of thickness, the highest average critical force value 2250 mN occurs when using an indenter with a rounding radius R of 200 um. It is three times higher than the average critical force values for the other three indenters (**Fig. 4a**). Such a large difference in the average critical values is due to the formation of initially elastic deformation followed by plastic deformation **[L. 15–18]**. When increasing the thickness of the coatings to 2 μm (2x), the highest critical force values occur for an indenter R equals to 500 μm (**Fig. 4b**). Compared to the other tested coatings with the same indenter geometry, this coating has the highest critical force value, which is 4000 mN (**Figs. 4b–f**). Further increase in coating thickness results in an increase

in coating stiffness, which ultimately leads to cracking and spalling of the coating.

When contacting a sample with an indenter of significantly smaller radius of rounding, the opposite situation can be observed (**Figs. 4a–f**). The highest value of the critical force when contacting an indenter R = 20 um for coating with thickness 5.2 um and 4.2 um is 399 mN and 250 mN respectively. The first permanent deformations appear directly in the coating at the interface between the coating and the indenter (**Fig. 4a**). This phenomenon can also be observed for the 2 µm coating (**Fig. 4b**).

The coating-substrate systems loaded by an indenter with a rounding radius R = 500 µm are 3.5 times higher than systems where an indenter present a rounding radius of 200 µm (**Fig. 4b**). For coatings with thickness 4.1 um and 5 um, the difference in average critical load values was also large and depended on the indenter rounding radius (**Figs. 4c–d**). Using an indenter with a rounded tip radius R = 20 µm, the force value for both coatings ranged between 200–400 mN. However, for the indenter with the largest round geometry, it was about three times higher and ranged from 700–1750 mN. The average critical load values for the thicker coatings are twice as low as for the thinner coatings. It can be observed because systems with thicker coating have higher stiffness. In addition, the stresses arising in the indenter axis and the substrate coating system are blocked at the surface and thus not transmitted to the substrate **[L. 16]** (**Figs. 4c–d**).

Cracks, depending on the contact geometry, can arise at the coating-substrate interface and propagate towards the coating surface or appear at the coating surface and propagate towards the substrate. The following figures show crack and deformation images of coating-substrate systems for 1–5.2 µm coatings at indenter radii ranging from 20 µm to 500 µm (**Fig. 5**). Deformation images were taken using a Micro Combi tester microscope at x500 magnification.

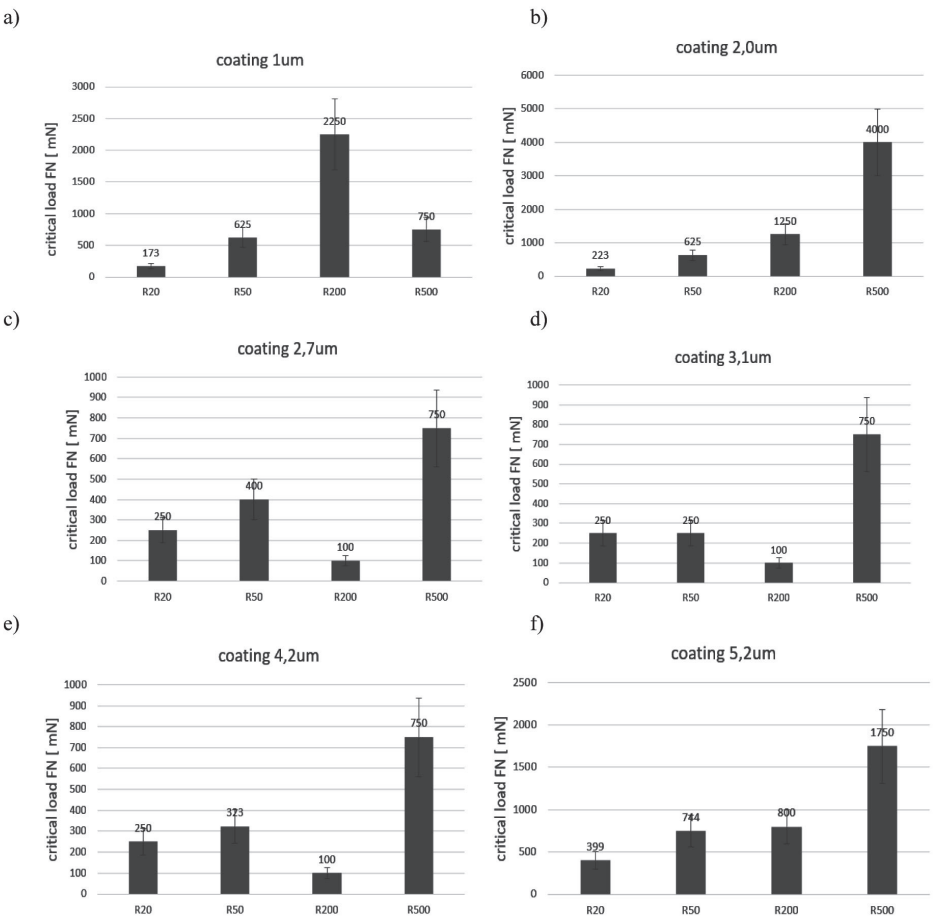

Fig. 4. The average value of the critical forces for various indenter geometry in the range of 20–500 µm for systems with different thicknesses of coatings: a) 1 µm, b) 2 µm, c) 2.7 µm, d) 3.1 µm, e) 4.2 µm, f) 4.2 µm

Rys. 4. Średnia wartość sił krytycznych dla różnych geometrii wgłębnika w zakresie 20–500 µm dla systemów o różnej grubości powłok: a) 1 µm, b) 2 µm, c) 2,7 µm, d) 3,1 µm e) 4,2 µm, f) 4,2 µm

The first cracks are formed at the periphery of the imprint just outside the contract zone for thin 1 and 2 μm coatings at an indenter geometry R of 20 μm. The maximum force at which this type of failure formation occurs ranges from 173––223 mN (**Fig. 5a**). A similar type of deformation of the coating-substrate system occurs at an indenter geometry of 50 μm (**Fig. 5b**) for thin coatings. For coatings with thicknesses of 4.1 and 5.2 μm, circumferential cracks arise outside the coating-indenter contact zone (**Fig. 5a–b**). Additionally, radial cracks also occur (**Figs. 5a–b**). These types of cracks cause peeling of the coating from the substrate and chipping leading to the exposure of the protected substrate **[L. 17]**. The situation was different for coating-substrate systems when indenters with larger geometries, i.e. 200 μm and 500 μm, were used (**Figs. 5c–d**). The first cracks are circumferential in nature, and are independent of the coating thickness. Crucial radial cracking does not occur here. However, at the interface between the coating and the substrate, plastic deformations occur **[L. 17–23]**, which cause cracking of the coating from the inside in the axis of the indenter contact with the system, especially for groups of coatings.

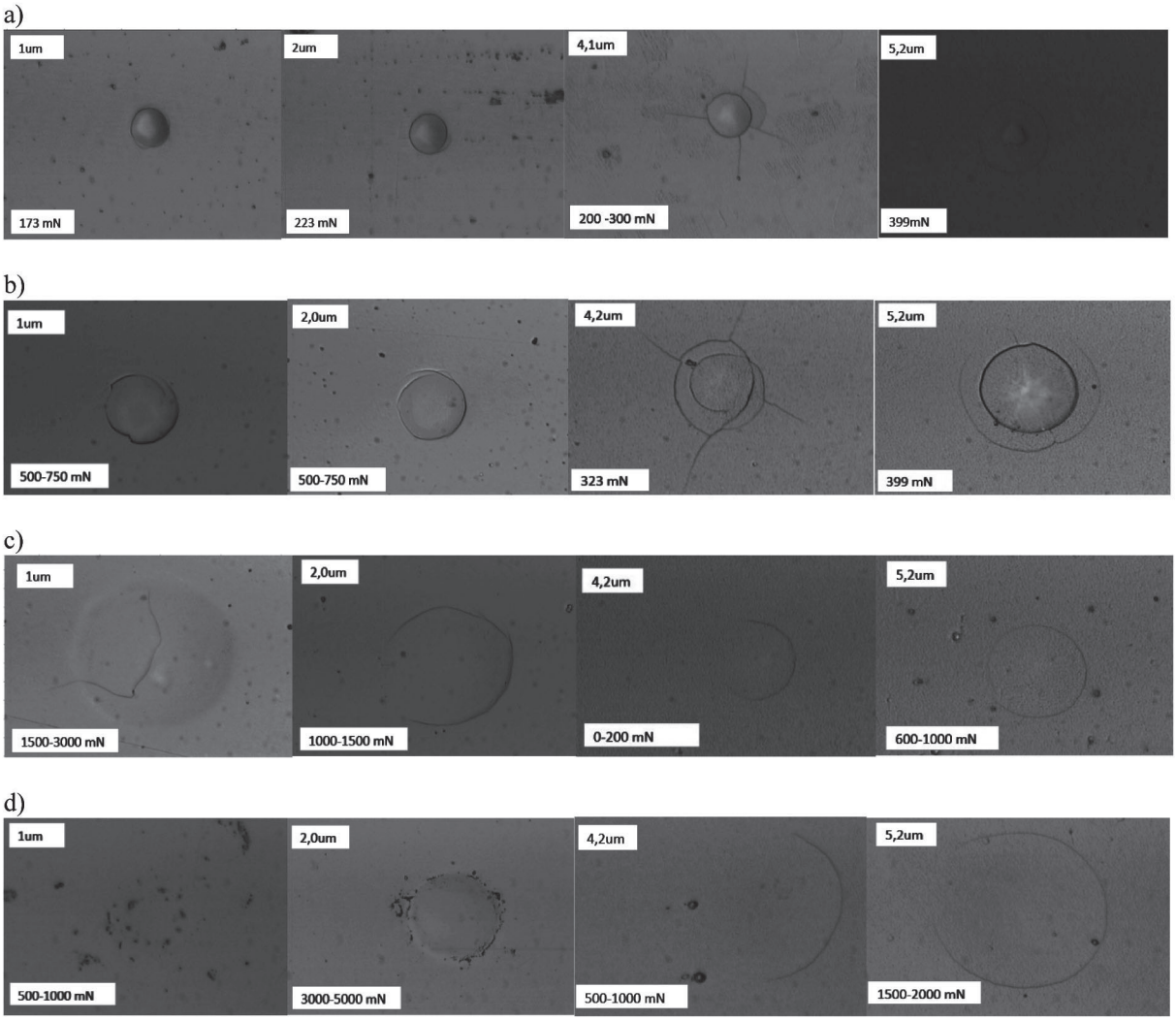

Fig. 5. Images of coating-substrate deformation using a Micro Combi Tester for an indenter with a fillet radius: a) R = 20 μm, b) R = 50 μm, c) R = 200 μm, d) R = 500 μm

Rys. 5. Obraz deformacji układu powłoka–podłoże przy użyciu Micro Combi Tester dla wgłębnika o promieniu zaokrąglenia: a) R = 20 μm, b) R = 50 μm, c) R = 200 μm, d) R = 500 μm

The images below present scanning electron microscope (SEM) images for the tested systems at maximum indenter loads of 1 N and 3 N (**Fig. 6**). The images represent crack propagation, i.e., the formation of cohesive and adhesion cracks occurring. Peripheral cracks in and out of the indenter axis are visible for coatings of 1.4 and 2.7 µm thickness and an indenter with a rounded radius R of 50 µm and 500 µm. These cracks are caused by circumferential stresses on the coating surface and at the coating-substrate interface (**Figs. 6a–b**). Using an indenter with a 500 µm radius of roundness, the formation of radial cracks was observed, which will cause delamination of the coating from the substrate when the load is increased (**Fig. 6b**) **[L. 16–18]**.

For thick coatings of 4.2 and 5.2 µm, the stresses at the coating-substrate interface are small when the substrate is plasticized **[L. 16–18]**. In contrast, a significant concentration of stresses can be observed at the coating surface (**Figs. 6c–d**). Circumferential cracks are formed in the contact axis and beyond the contact zone. Subsequent circumferential cracks are located further away than circumferential cracks in thin coatings. This indicates that thick coatings at very high loads are more susceptible to brittle fracture than thin coatings. The SEM images also show radial cracks, which are very dangerous. They cause separation of the coating from the substrate, which results in the lack of protection of the surface against destructive loads.

The most commonly observed forms of damage to the coating-substrate system are analysed at elastic deformation and beyond its limit when plasticization of the coating or substrate occurs. In the optical profilometer images, the curvature of the coating outflow can be seen beyond the 1.4 µm and 4.2 µm indenter-coating contact zones (**Fig. 7**). For the first case, where an indenter with

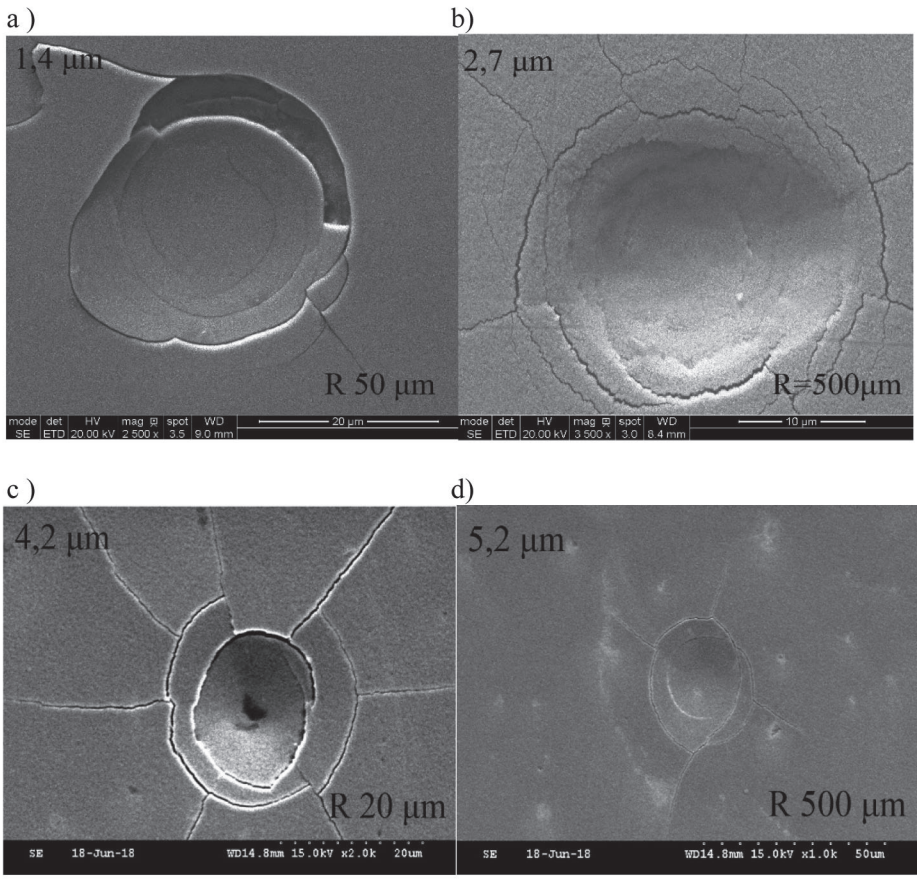

Fig. 6. Images of cracks using the SEM scanning electron microscope at maximum load 3 N for coatings with thickness: a) 1.4 µm, b) 2.7 µm, c) 4.2 µm, d) 5.2 µm

Rys. 6. Obraz pęknięć przy użyciu skaningowego mikroskopu elektronowego SEM przy maksymalnym obciążeniu 3 N dla powłok o grubości: a) 1,4 µm, b) 2,7 µm, c) 4,2 µm, d) 5,2 µm

a rounded tip radius of 20 µm was used, a much larger radius of rounding of the bead is visible (**Fig. 7**). Initially, the elastic nature of the deformation can be observed for both indenters. In contrast, it can be seen precisely that using an indenter with a smaller geometry results in more plasticization of the coating than when using the R 500 µm indenter for thick coatings (**Fig. 7**). Due to the stiffness of the system, the radius of rounding of the flotation is smaller than for a thinner coating and smaller rounded tip geometry (**Fig. 7b**) **[L. 16–18]**.

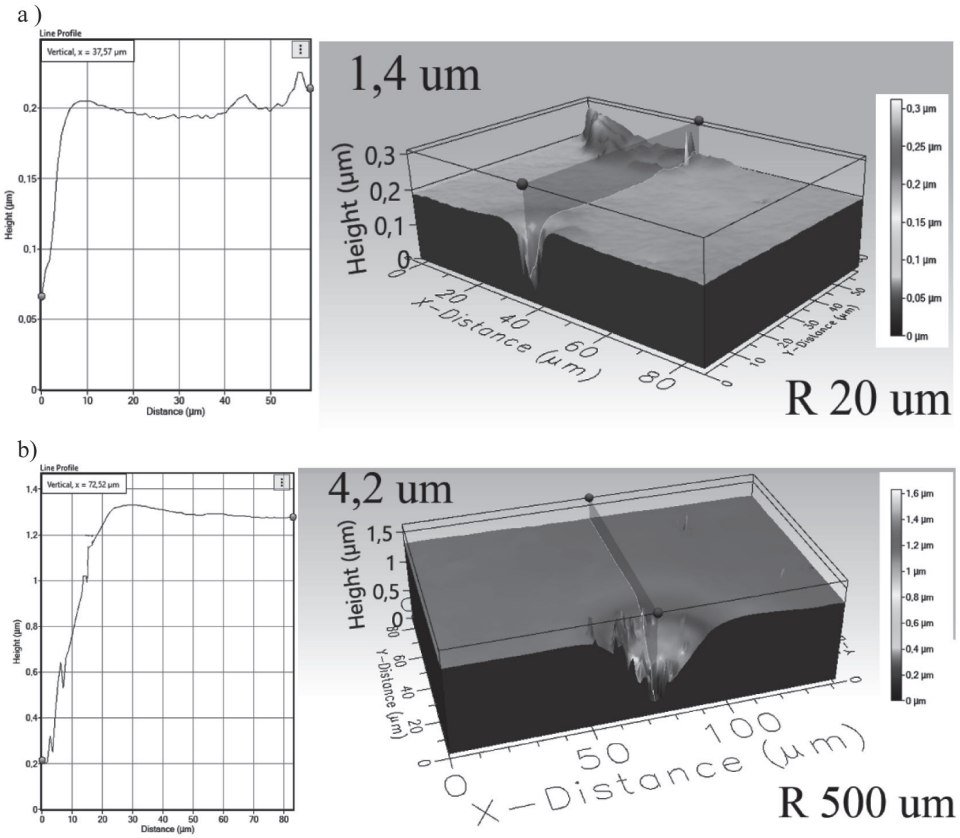

Fig. 7. Images of deformation of the coating-substrate system at average values of the critical load: a) diagram of the penetration depth of the indenter for the thickness coating 1.4 µm and the rounding radius of indenter R = 20 µm, b) diagram of the penetration depth of the indenter for the thickness coating R = 4.2 µm and the rounding radius of indenter R = 500 µm

Rys. 7. Obrazy deformacji układu powłoka–podłoże przy średnich wartościach obciążenia krytycznego: a) wykres głębokości penetracji wgłębnika dla grubości powłoki 1,4 µm i promienia zaokrąglenia wgłębnika R = 20 µm, b) wykres głębokości penetracji wgłębnika dla grubości powłoki R = 4,2 µm i promienia zaokrąglenia wgłębnika R = 500 µm

CONCLUSIONS

Determination of permissible loads is extremely important for tribological applications of elements to which coatings are deposited. Interaction of friction pairs under loads lower than permissible significantly extends the life-time operation of machines. Wear of tribological pairs occurs as a result of abrasive wear without the formation of cracks or the separation of the coating from the substrate, which leads to a faster destruction of the machine.

The proposed method of instrumental indentation, analysis of scanning electron microscope, and optical profilometer images allow to determining the average values of critical loads, after exceeding which various forms of system destruction occur.

By analyzing the resulting deformations, it is possible to determine the character of the system for the studied coating-substrate systems experimentally. Determination of these loads in an analytical manner is practically impossible due to the complex state of stresses in such systems.

REFERENCES

1. Kot M.: An Analysis of Mechanical and Tribological Properties of Zr/Zr_2N Multilayer Coatings, Archives of Civil and Mechanical Engineering, 12, 2022, pp. 464–470.
2. Kot M., Moskalewicz T., Wendler B., Rakowski W., Czyrska-Filemonowicz A.: Micromechanical and tribological properties of nc-TiC/a-C nanocomposite coatings, Solid State Phenomena, 177, 2011, pp. 36–46.
3. Burakowski T., Wierzchoń T.: Inżynieriia powierzchni metali. Wydawnictwo Naukowo-Techniczne, Warszawa 1995, pp. 47–61, 191–219, 449–550.
4. Dobrzański L.A, Dobrzańska-Danikiewicz A.D.: Obróbka powierzchni metali inżynierskich. Opem Access Library, 2011, pp. 89–136.
5. Hebda M., Wachgal A.: Tribologia. Wydawnictwo Naukowo-Techniczne, Warszawa 1980, pp. 468–533.
6. Kot M., Rakowski W., Morgiel J., Major Ł.: Metoda wyznaczania nacisków dopuszczalnych w styku skoncentrowanym dla układów powłoka–podłoże. Tribologia, 2018, pp. 285–295.
7. Herbert E.G., Pharr G.M., Olivier W.C., Lucas B.N, Hay J.L.: On the measurement of stress-strain curves by spherical indentation. Thin Solid Dilms, 2001, pp. 331–335.
8. Kot M., Rakowski W., Morgiel J., Major Ł.: Load-bearing capacity of coating- substrate systems obtained from spherical indentation tests. Thin Solids Films, 2013, pp. 345–355.
9. Ullner C., Beckmann J., Morrell R.: Instrumented indentation test for advanced technical ceramics. Journal of the European Ceramic, Society, 2002, pp. 1183–1189.
10. Fernandes J.V., Trindade A.C, MenezesS L.F., Cavalwiro A.: A model for coated surface hardness. Surface and Coatings Technology 131, 2000, pp. 457–461.
11. ISO 14577-1. Metallic materials – instrumented indentation test for hardness and material parameters – Part 1: Test method.
12. ISO 20808:2004. Fine ceramics (advanced ceramics, advanced technical ceramics) – Determination of friction and wear characteristics of monolithic ceramics by ball-on-disc method.
13. Chronowska-Przywara K., Kot M., Zimowski S.: Technika badawcze w analizie własciwości mechanicznych i tribologicznych cienkich warstw i powłok. Zesyty naukowe Politechniki Śląskiej. Seria Transport z.83, (2014).
14. Wiciński Pp. Smolik J., Garbacz H.: Microstructure and mechanical properties of nanostructure multilayer CrN/Cr coatings on titanium Alloy. Thin Solid Films vol. 519, issue 12. 2011, pp. 4069–4073.
15. Chronowska-Przywara K., Kot M.: Modelowanie metodą elementów skończonych deformacji i naprężeń układu powłoka–podłoże w teście zarysowania, Tribologia: teoria i praktyka, 2015, pp. 33–43.
16. Kot M.: Deformacje i pękanie układów powłoka–podłoże przy obciążeniach działających w styku skoncentrowanym. Tribologia: Teoria i praktyka, 2010, pp. 125–133.
17. Chronowska-Przywara K., Kot M., Szczęch M.: The effect of residual stress of the load bearing capacity of PVD coated surfaces – part 2, Tribologia: teoria i praktyka, 5–2019, pp. 43–49.
18. Chronowska-Przywara K., Kot M., Szczęch M., The effect of residual stress of the load bearing capacity of PVD coated surfaces – part 2, Tribologia: teoria i praktyka, 4–2018, pp. 23–29.
19. John A. Williams, Rob S. Dwyer-Joyce: Modern Tribology Handbook – Contact between solid surfaces, CRC Press LLC, 2001, pp. 1432–1468.
20. Wang T., Wang L., Zheng L.G.: Stress analysis of elastic coated solids in point contact, Tribology International 86, 2015, pp. 52–61.
21. Steve G., Charles W., Yordanos B.: Determination of residual stress in brittle materials by Hertzian indentation: Theory and experiment, Journal of the American Ceramic Society, vol. 82, 1999, pp. 125–132.
22. Tang K.C., Faulkner A., Schwarzer N., Arnell R.D., Richter F.: Comparison between an elastic-perfectly plastic finite element model and a purely elastic analytical model for a spherical indenter on a layered substrate, Elsevier. Thin Solid Films, 1997, pp. 177–188.
23. Muchler J., Blank E.: Analysis of coating fracture and substrate plasticity induced by spherical indentors: diamond and diamond – like – carbon layers on steel substrates, Elsevier. Thin solid Films, 2001, pp. 119–134.